# Melanoma

# 11

Daniela Hartmann

Fast diagnostic methods in melanoma have been gaining importance in the last few decades due its malignant nature and its rising incidence [1]. Being able to safely distinguish normal or dysplastic nevi from melanoma intraoperatively and immediately decide further therapeutic steps would potentially decrease the number of surgical procedures [2], as well as associated risk of complications. Possible use of ex vivo confocal laser scanning microscopy (ex vivo CLSM) in melanoma diagnostics, including fast immunofluorescence [3] and intraoperative tumor thickness measurement [4], as well as up-to-date experience (Table 11.1) together with examples of melanoma images (Figs. 11.1, 11.2, 11.3 and 11.4) are presented and discussed.

## 11.1 Basics of Melanoma

- Definition: Malignant, invasive melanocytic skin tumor clinically presenting mostly as a deep brown to blue-blackish, brown-reddish, or even pigment-free (amelanotic melanoma) nodule or plaque with an early tendency to metastasize (strongly depending on tumor thickness). Different types of melanoma are distinguished on the basis of clinical and histological criteria (superficial spreading melanoma, nodular melanoma, lentigo maligna melanoma, acral lentiginous melanoma, and others) [1].
- Epidemiology: The incidence in a fair skinned population in Europe and North America is estimated to be 15/100,000 people annually [1].
- Histopathology: Melanomas have various histologic features including presence of atypical melanocytes singly or as nests with varying shape and size. These atypical cells can invade local structures causing their destruction. Atypical mitosis in the tumor cells, trans-epidermal melanocytic migration (TEM), asymmetry of the tumor, ill-defined tumor, horizontal confluence of the nests, lack of maturation of tumor cells in the deep dermis, vascular and/or perineural invasion, as well as spread of melanoma nests along the epithelial adnexal structures. Ulceration of the tumor, solar elastosis in the dermis, and strong peritumoral inflammatory infiltrate may occur [5].
- Immunofluorescence: First pilot studies on the combination of ex vivo CLSM and fluorescent-tagged antibodies have indicated new opportunities for fast and specific tissue examination [3, 6–11]. There is a particular interest in developing such techniques for the examination of melanocytic lesions to distinguish malignant from benign lesions. First report on the use of fluorescent-tagged S100-antibody and fluorescent-tagged Melan-A-antibody proved the possibility of such a concept and at the same time showed the complexity of such implementation within intraoperative setting [3]. Further studies on the use of immunofluorescence in the ex vivo CLSM are necessary.
- Confocal tumor thickness MEASUREMENT: Ex vivo CLSM enables intraoperative measurement of tumor thickness. First pilot study showed promising results and very good correlations to the tumor thickness on histopathology tissue Sect. (4). Larger studies on confocal tumor thickness measurement are needed to validate these results.

D. Hartmann (✉)
Department of Dermatology and Allergy, University Hospital, LMU Munich Frauenlobstrasse, 9-11, 80337 Munich, Germany
e-mail: Daniela.Hartmann@med.uni-muenchen.de



M. Jain et al. (eds.), *Cutaneous Atlas of Ex Vivo Confocal Microscopy*,
https://doi.org/10.1007/978-3-030-89316-3_11

**Table 11.1** Melanoma features on FCM, DHE, and corresponding conventional H&E

| In cases of melanomas, especially arising in nevi, all normal and/or dysplastic melanocytic nevi features described in Chaps. 9 and 10 may occur. Additional features often found in melanoma are listed below | | |
|---|---|---|
| Fluorescence confocal microscopy mode (FCM) mode (green scale images) [2] | Digital H&E (combined FCM and RCM modes) | Conventional H&E-stained images |
| **Fluorescence in the epidermis**: Nuclei of the tumor cells visualized as bright white (green*) dots of variable shape, brightness and sizes ascending in the epidermis and/or spread throughout the entire epidermis (Figs. 11.1 and 11.2) | The bright white (green*) dots on FCM appear dark purple (high fluorescence signal) or dark to light pink (low fluorescence signal; dominant reflectance signal) on DHE. The tumor cells are ascending throughout or infiltrating the whole epidermis. The variable cell size may be better visible in DHE than in FCM | Atypical melanocytes with TEM and/or consumption of the epidermis by atypical melanocytes |
| **Fluorescence in the dermo-epidermal junction and dermis**: White (green*) 'tongues' of the epidermis of variable shape and brightness, interconnected horizontally at the dermo-epidermal junction and/or papillary dermis (Figs. 11.1 and 11.2) | Dark purple to dark pink 'tongues' of the epidermis of variable shape and brightness, interconnected horizontally at the dermo-epidermal junction and/or papillary dermis | Atypical melanocytic nests with horizontal confluence |
| **Fluorescence in the epithelial adnexal structures (e.g. hair follicles)**: Bright white (green*) dots of variable shape, brightness and sizes spreading along the epithelium of the adnexal structures ( Fig. 11.1) | Dark purple dots, surrounded by light purple to pink cytoplasm, of variable shape and sizes spreading along the epithelial adnexal structures | Spread of melanoma cells and/or nests along the epithelium of the adnexal structures |
| **Fluorescent structures in the dermis and subcutis**: Homogeneous, greyish (light to dark green*), slightly shining structureless mass (Fig. 11.1) | Homogeneous, light to dark purple structureless mass | Solar elastosis |
| **Other fluorescent structures in the dermis and subcutis**: Heterogeneous nests of varying shape, sizes and brightness consisting of atypical melanocytes in shades of grey (light to dark green*) (Fig. 11.3) | Heterogeneous purple to pink nests of varying shapes and sizes consisting of atypical melanocytes | Dermal nests of atypical melanocytes showing cellular and nuclear polymorphism without sign of maturation |
| **Nuclear fluorescent structures**: Bizarre shaped bright white (bright green*) chromatin structures in the nuclei (Fig. 11.4) | Bizarre shaped dark purple chromatin structures in the nuclei | Atypical mitosis in the melanoma cells |

FCM = fluorescent confocal microscopy, DHE = digital hematoxylin–eosin-like staining, H&E = hematoxylin–eosin staining, TEM = trans-epidermal melanocytic migration, * color of the fluorescent signal depending on the generation of the ex vivo CLSM device

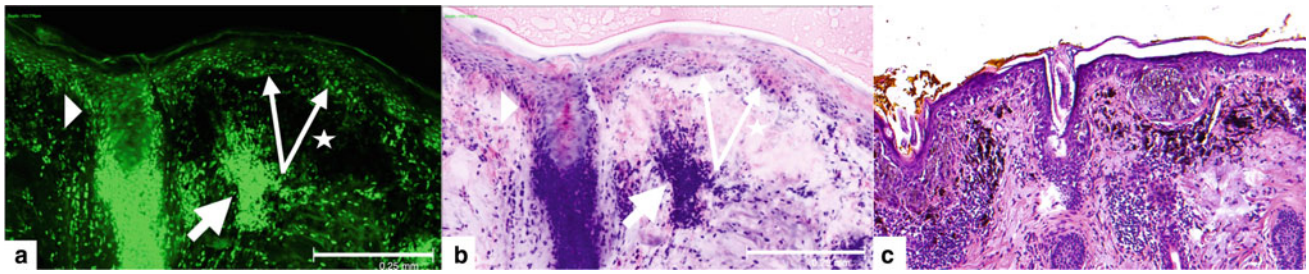


**Fig. 11.1** Superficial spreading melanoma examined in two modes of the ex vivo confocal laser scanning microscopy (**a** fluorescence, **b** DHE), and comparison with their corresponding H&E-stained image (c) presenting nests of varying size and shape consisting of atypical melanocytes in the epidermis and dermo-epidermal junction (long arrow), as well as strong inflammatory infiltrate (short, thick arrow), and solar elastosis (star) in the dermis. Melanocytic spread along the follicle is highlighted with an arrowhead. DHE = digital hematoxylin–eosin-like staining. H&E magnification = 10x

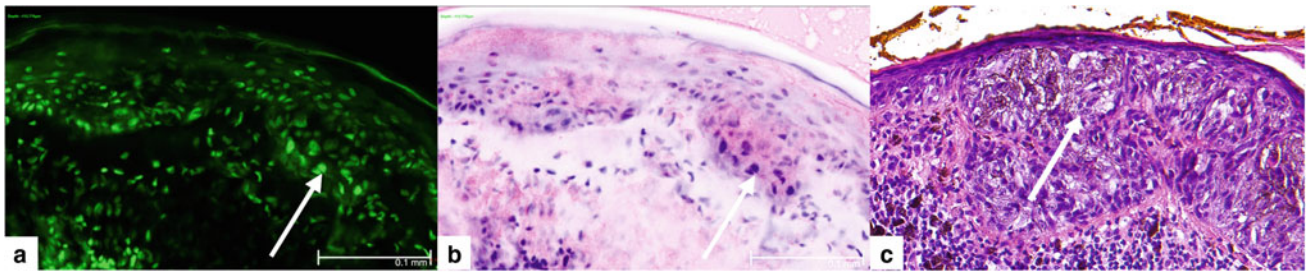


**Fig. 11.2** Detailed view of a superficial spreading melanoma examined in two modes of the ex vivo confocal laser scanning microscopy (**a** fluorescence, **b** DHE) and comparison with their corresponding H&E-stained image (**c**), presenting atypical melanocytes clustered in nests as well as single cell proliferates in the epidermis and dermo-epidermal junction (long arrow) showing signs of transepidermal melanocytic migration DHE = digital hematoxylin–eosin-like staining. H&E magnification = 20x

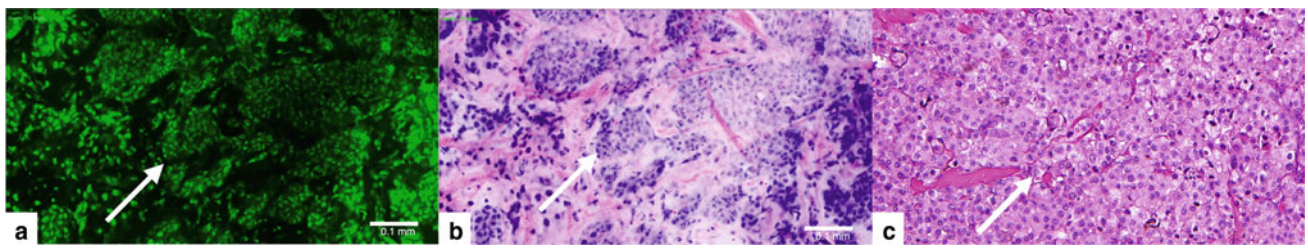


**Fig. 11.3** Dermal part of a nodular melanoma examined in two modes of the ex vivo confocal laser scanning microscopy (**a** fluorescence, **b** DHE) and comparison with their corresponding H&E-stained image (**c**), presenting dermal nests of varying size and shape consisting of atypical melanocytes (arrow) showing varying levels of fluorescence signal, as well as cellular and nuclear pleomorphism. DHE = digital hematoxylin–eosin-like staining. H&E magnification = 20x

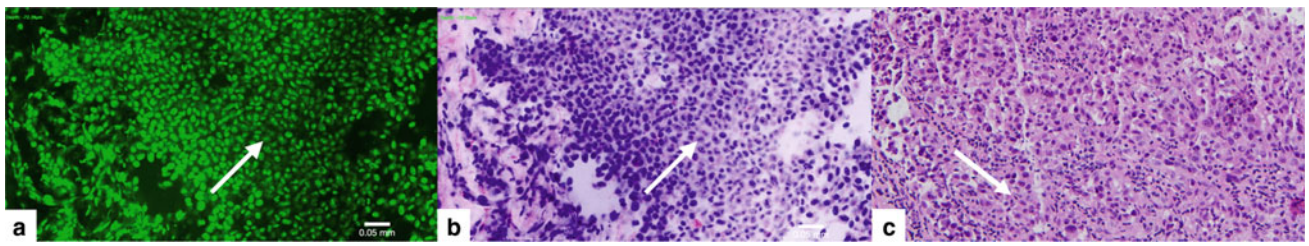


**Fig. 11.4** Melanoma metastasis examined in two modes of the ex vivo confocal laser scanning microscopy (**a** fluorescence, **b** DHE) and comparison with their corresponding H&E-stained image (**c**), presenting masses of atypical melanocytes (arrow) with multiple atypical mitoses. DHE = digital hematoxylin–eosin-like staining. H&E magnification = 20x

## References


1. Leitlinienprogramm Onkologie. Deutsche Krebsgesellschaft, Deutsche Krebshilfe, AWMF. S3-Leitlinie Prävention von Hautkrebs, Langversion 1.1. 2014. http://leitlinienprogramm-onkologie.de/Leitlinien.7.0.html. Accessed 03 Feb 2021.
2. Hartmann D, Ruini C, Mathemeier L, Bachmann MR, Dietrich A, Ruzicka T, von Braunmühl T. Identification of ex-vivo confocal laser scanning microscopic features of melanocytic lesions and their histological correlates. J Biophotonics. 2017;10(1):128–42.
3. Hartmann D, Krammer S, Vural S, Bachmann MR, Ruini C, Sárdy M, Ruzicka T, Berking C, von Braunmühl T. Immunofluorescence and confocal microscopy for ex-vivo diagnosis of melanocytic and non-melanocytic skin tumors: A pilot study. J Biophotonics. 2018 Mar;11(3).
4. Hartmann D, Krammer S, Ruini C, Ruzicka T, von Braunmühl T. Correlation of histological and ex-vivo confocal tumor thickness in malignant melanoma. Lasers Med Sci. 2016;31(5):921–7.
5. Wade TR, White CR Jr. The histology of malignant melanoma. Med Clin North Am. 1986;70(1):57–70.
6. Bağcı IS, Aoki R, Krammer S, Ruzicka T, Sárdy M, Hartmann D. Ex vivo confocal laser scanning microscopy: An innovative method for direct immunofluorescence of cutaneous vasculitis. J Biophotonics. 2019 Sep;12(9):e201800425.
7. Bağcı IS, Aoki R, Krammer S, Ruzicka T, Sárdy M, French LE, Hartmann D. Ex vivo confocal laser scanning microscopy for bullous pemphigoid diagnostics: new era in direct immunofluorescence? J Eur Acad Dermatol Venereol. 2019;33(11):2123–30.
8. Krammer S, Krammer C, Salzer S, Bağci IS, French LE, Hartmann D. Recurrence of Pemphigus Vulgaris Under Nivolumab Therapy. Front Med (Lausanne). 2019;12(6):262.
9. Bağcı IS, Aoki R, Krammer S, Vladimirova G, Ruzicka T, Sárdy M, French LE, Hartmann D. Immunofluorescence and histopathological assessment using ex vivo confocal laser scanning microscopy in lichen planus. J Biophotonics. 2020 Dec;13(12):e202000328.
10. Bağcı IS, Aoki R, Vladimirova G, Ergün E, Ruzicka T, Sárdy M, French LE, Hartmann D. New-generation diagnostics in inflammatory skin diseases: Immunofluorescence and histopathological assessment using ex vivo confocal laser scanning microscopy in cutaneous lupus erythematosus. Exp Dermatol. 2020 Dec 21.
11. Bağcı IS, Aoki R, Vladimirova G, Sárdy M, Ruzicka T, French LE, Hartmann D. Simultaneous immunofluorescence and histology in pemphigus vulgaris using ex vivo confocal laser scanning microscopy. J Biophotonics. 2021 Jan 24:e202000509.